© 2017. Published by The Company of Biologists Ltd | Journal of Cell Science (2017) 130, 2159-2171 doi:10.1242/jcs.200634

RESEARCH ARTICLE

A Wntless–SEC12 complex on the ER membrane regulates early Wnt secretory vesicle assembly and mature ligand export

Jiaxin Sun[1], Shiyan Yu[1], Xiao Zhang[1], Catherine Capac[1], Onyedikachi Aligbe[1], Timothy Daudelin[1], Edward M. Bonder[1] and Nan Gao[1,2,*]

ABSTRACT

Wntless (Wls) transports Wnt molecules for secretion; however, the cellular mechanism underlying the initial assembly of Wnt secretory vesicles is still not fully defined. Here, we performed proteomic and mutagenic analyses of mammalian Wls, and report a mechanism for formation of early Wnt secretory vesicles on ER membrane. Wls forms a complex with SEC12 (also known as PREB), an ER membrane-localized guanine nucleotide-exchange factor (GEF) activator of the SAR1 (the SAR1A isoform) small GTPase. Compared to palmitoylation-deficient Wnt molecules, binding of mature Wnt to Wls increases Wls–SEC12 interaction and promotes association of Wls with SAR1, the key activator of the COPII machinery. Incorporation of Wls into this exporting ER compartment is affected by Wnt ligand binding and SEC12 binding to Wls, as well as the structural integrity and, potentially, the folding of the cytosolic tail of Wls. In contrast, Wls–SEC12 binding is stable, with the interacting interface biochemically mapped to cytosolic segments of individual proteins. Mutant Wls that fails to communicate with the COPII machinery cannot effectively support Wnt secretion. These data suggest that formation of early Wnt secretory vesicles is carefully regulated to ensure proper export of functional ligands.

KEY WORDS: Wnt, Wntless, Wls, Secretion, SAR1, SEC12, COPII

INTRODUCTION

Wnts are secreted glycolipoproteins that are fundamental for embryonic development and adult tissue homeostasis (Feng and Gao, 2015; Herr et al., 2012). Abnormal Wnt signal transduction in cells is associated with human diseases and, in particular, colorectal cancers (Clevers and Nusse, 2012). Certain cancer cells exhibit enhanced Wnt production (Voloshanenko et al., 2013). Small molecules that target Wnt secretion in advanced solid tumors show promising inhibitory effects (Duraiswamy et al., 2015; Liu et al., 2013; Madan et al., 2016), and multiple clinical trials (NLM numbers NCT01351103, NCT02278133 and NCT02521844) are ongoing to determine the efficacy and toxicity of these Wnt secretory inhibitors. Thus, it is imperative to gain a better understanding of the molecular basis of Wnt secretion.

In Wnt-secreting cells, newly synthesized ligands are initially palmitoylated by the endoplasmic reticulum (ER) membrane-bound O-acyltransferase Porcupine (Porcn) (Gao and Hannoush, 2014; Kurayoshi et al., 2007). Human and mouse Porcn specifically lipidates Wnt3a at serine 209 (Coombs et al., 2010; Herr and Basler, 2012; Janda et al., 2012; MacDonald et al., 2014; Takada et al., 2006; Willert et al., 2003). Lipidated Wnts are then transported by an evolutionarily conserved multi-pass transmembrane protein called Wntless (Wls) (also known as Mig-14 in *C. elegans* and Gpr177 in mice) for exocytosis (Banziger et al., 2006; Bartscherer et al., 2006; Goodman et al., 2006). Loss-of-function studies affirmed the indispensable role of Wls for secretion of virtually all Wnts across the animal kingdom (Banziger et al., 2006; Bartscherer et al., 2006; Fu et al., 2009). Interestingly, in Porcn-deficient cells, non-lipidated Wnts cannot be recognized and transported by Wls, resulting in ligand accumulation in ER (Herr and Basler, 2012; Proffitt et al., 2013).

After Wnts are released from the secreting cells to extracellular matrix, Wls is internalized from the plasma membrane via AP2- and clathrin-dependent pathways to endosomes (Gasnereau et al., 2011; Pan et al., 2008), where Wls is retrieved by retromer, in a Vps35- and SNX3-dependent fashion, to the Golgi (Belenkaya et al., 2008; Franch-Marro et al., 2008; Harterink et al., 2011; Port et al., 2008; Rojas et al., 2008; Yang et al., 2008). Sorting of ligand-bound Wls from endosomes to multivesicular bodies (MVBs) has been shown to lead to exosome-mediated export of unsecreted Wnts that remain with Wls (Gross et al., 2012). Recent studies further illustrated the involvement of ARF/ERGIC2 and COPI vesicles in regulating a further retrograde transport of Wls from the Golgi to the ER for new rounds of Wnt transport (Yu et al., 2014a). These studies highlighted a sophisticated regulation of retrograde Wls traffic, which is presumably designed for reusing the transporter for an effective Wnt export.

In contrast to the retrograde Wls trafficking, little to nothing is currently known about how Wls–Wnt is exported from ER and subsequently delivered to plasma membrane for exocytosis (Das et al., 2012). A genome-wide RNAi screen for Wg secretion in *Drosophila* suggested the potential involvement of two p24 family proteins, Emp24 (also known as CG9308) and Éclair, in ER export of Wg (Port et al., 2011). Another p24 family protein, CG9053, known as Opossum in flies, was also proposed to affect the ER-to-Golgi transport of Wg, as Wg accumulated in ER in its absence (Buechling et al., 2011). Biochemical interactions between Wg and Emp24 or Opossum in *Drosophila* suggest that a certain degree of regulation exists for the step where the ligand exits the ER (Buechling et al., 2011; Li et al., 2015). It was important to note that above studies on Wg and p24 proteins shed little light on the functional contribution of Wls to this particular process of Wg export. We recently reported that the mammalian Wls travels through Rab8a-positive vesicles as part of the Wnt secretion process. Loss of Rab8a weakens Wnt production *in vitro* and *in vivo*, impacting Paneth cell maturation in mouse intestinal crypts (Das et al., 2015). However, additional key molecular machinery that controls the anterograde Wls–Wnt traffic remains to be explored.

[1]Department of Biological Sciences, Rutgers University, Newark, NJ, USA.
[2]Rutgers Cancer Institute of New Jersey, Rutgers University, Piscataway, NJ, USA.

*Author for correspondence (ngao@rutgers.edu)

N.G., 0000-0003-4264-7438

Received 12 December 2016; Accepted 11 May 2017

Journal of Cell Science (2017) 130, 2159-2171 doi:10.1242/jcs.200634

Here, we report a previously undescribed mechanism for formation of early Wnt secretory vesicle on ER membrane. Proteomic analysis of wild-type and a traffic-defective Wls uncovered the involvement of COPII complex in ER export of Wls. We identified a stable interaction between Wls and SEC12 (also known as PREB), an ER membrane-localized guanine nucleotide-exchange factor (GEF) for the SAR1 (the SAR1A isoform) small GTPase, and biochemically mapped the interacting surfaces to specific cytosolic motifs in individual proteins. Wls-SEC12 interaction was necessary for Wls association with SAR1 and incorporation to COPII complex. Binding of mature Wnt to Wls enhanced Wls–SEC12 complex formation, and promoted Wls–SAR1 association. Wls incorporation into COPII compartment appeared to be sensitively dependent on Wnt–Wls binding, SEC12–Wls binding, and the structural integrity of Wls cytosolic tail. Our data suggest that the formation of nascent Wnt secretory vesicle is regulated by ER export machinery to ensure delivery of mature ligands.

RESULTS

Proteomic analysis uncovers the involvement of COPII machinery in Wls trafficking

We previously showed that a C-terminally truncated mouse Wls (amino acids 1–491) failed to enter the secretory pathway (Das et al., 2015). We hypothesized that a proteomic analysis comparing wild-type Wls and this trafficking-defective Wls^{1-491} might shed light on cellular machineries that regulate Wls trafficking. An N-terminally Flag-tagged full-length Wls has been described in biochemical and functional Wnt secretion studies in cultured cells (Jin et al., 2010). Using an anti-Flag antibody, we performed immunoprecipitation (IP) on HeLa cells stably expressing 3×Flag-tagged full-length Wls or Wls^{1-491}. The precipitates were resolved by SDS-PAGE, and subjected to in-gel digestion followed by mass spectrometry identification. Proteomic analysis for interactors with wild-type Wls affirmed a number of previously reported regulators of Wls trafficking, including proteins associated with secretory vesicles (Rab8a) (Das et al., 2015), endosomes [adaptor protein (AP) 2] (Pan et al., 2008), as well as clathrin (Gasnereau et al., 2011) and retromer (VPS26, VPS29 and VPS35) (Port et al., 2008) (Table 1). In contrast, proteomic analysis of interactors for Wls^{1-491} showed an almost complete loss of the above factors, consistent with the defective vesicular trafficking of Wls^{1-491}. However, ER-resident proteins, as well as Wls itself, were detected in the Flag–Wls^{1-491} proteomic analysis (Table 1), suggesting that a lack of detected vesicular trafficking regulators in Wls^{1-491} precipitates was not due to degradation of this mutant.

Importantly, proteomic analysis of wild-type Wls interactors uncovered several major components of the COPII machinery, including the COPII-specific small GTPase (SAR1), inner coat proteins (SEC23 and SEC24), outer coat proteins (SEC31), and COPII-specific adaptors (TMED7, TMED9 and TMED10) (the specific SEC protein isoforms found are shown in Table 1). None of these COPII proteins was present in Wls^{1-491} precipitates. Co-IP analysis validated the specific associations of wild-type Flag–Wls, but not Wls^{1-491}, with SAR1, SEC24B and TMED10 (Fig. 1A). In addition, we observed an interaction between Wls and SEC12, the specific GEF activator of SAR1. Wls^{1-491} also binds to SEC12. These data indicated that Wls might travel through COPII vesicles for Wnt export (Fig. 1B). The loss of cytosolic tail in Wls^{1-491} most likely prevented its incorporation into COPII vesicles due to a potential misfolding or lack of association with COPII machinery. Our proteomic study did not identify any components of the ER-to-Golgi intermediate complex that regulates an alternative ER-to-Golgi transport pathway, suggesting that Wls may selectively utilize COPII vesicles for ER exit.

Table 1. Proteomic identification of protein targets in wild-type Wls and Wls^{1-491} immunoprecipitates

Cellular compartment and identified proteins	Spectra counts (number of unique peptides)	
	Wild-type Wls	Wls^{1-491}
ER		
Wls	17 (7)	19 (7)
CALL	9 (4)	13 (5)
HSP 90	32 (7)	19 (8)
HSP70C	57 (28)	33 (25)
Lysosome		
LAMP1	5 (4)	5 (4)
LAMP2	6 (3)	5 (2)
Golgi		
AP1	10 (7)	2 (2)
p115	2 (2)	0
GOGA4	1	0
ACBD3	2 (2)	0
COPII complex		
SEC23B	4 (3)	0
SEC24C	6 (4)	0
SEC31A	1	0
SAR1	1	0
TMED7	1	0
TMED9	3 (2)	0
TMED10	2 (2)	0
Known Wls-interacting proteins		
RAB8A	7 (1)	0
AP2M1	2 (2)	0
AP2A1	1	0
VPS29	1	0
VPS26A	1	0
VPS35	5 (5)	0
Clathrin	56 (39)	1
Rab small GTPases		
RAB18	1	0
RAB21	1	0
RAB38	2 (2)	0
RAB25	3 (2)	0
RAB5C	5 (2)	0
RAB3D	4 (1)	0
RAB5A	6 (4)	1
RAB2A	6 (6)	0
RAB11A	7 (5)	0
RAB10	7 (1)	0
RAB1B	8 (4)	0
RAB14	9 (6)	0
RAB7A	10 (6)	0
RAB9A	1	0

Note that protein bands corresponding to antibody heavy chain (~50 kDa), detected by Ruby protein stain, were excised and excluded from the analysis. This exclusion might have caused the elimination of SEC12 (runs at ~46 kDa) in proteomic identification.

Export of Wls into COPII vesicles depends on SAR1 activity

Formation and release of COPII vesicles from ER membrane are driven by the GTP/GDP exchanging dynamics of SAR1 (Sato and Nakano, 2005). In general, SEC16 recruits SEC12 to ER exit sites (Montegna et al., 2012). SEC12 resides in ER membrane as a single-pass transmembrane protein, which recruits and stimulates SAR1 activity as a specific GEF (Barlowe and Schekman, 1993). GTP-loaded active SAR1 attaches to the ER membrane (Aridor et al., 2001), initiating a sequential assembly of inner (SEC23–SEC24)

Journal of Cell Science (2017) 130, 2159-2171 doi:10.1242/jcs.200634

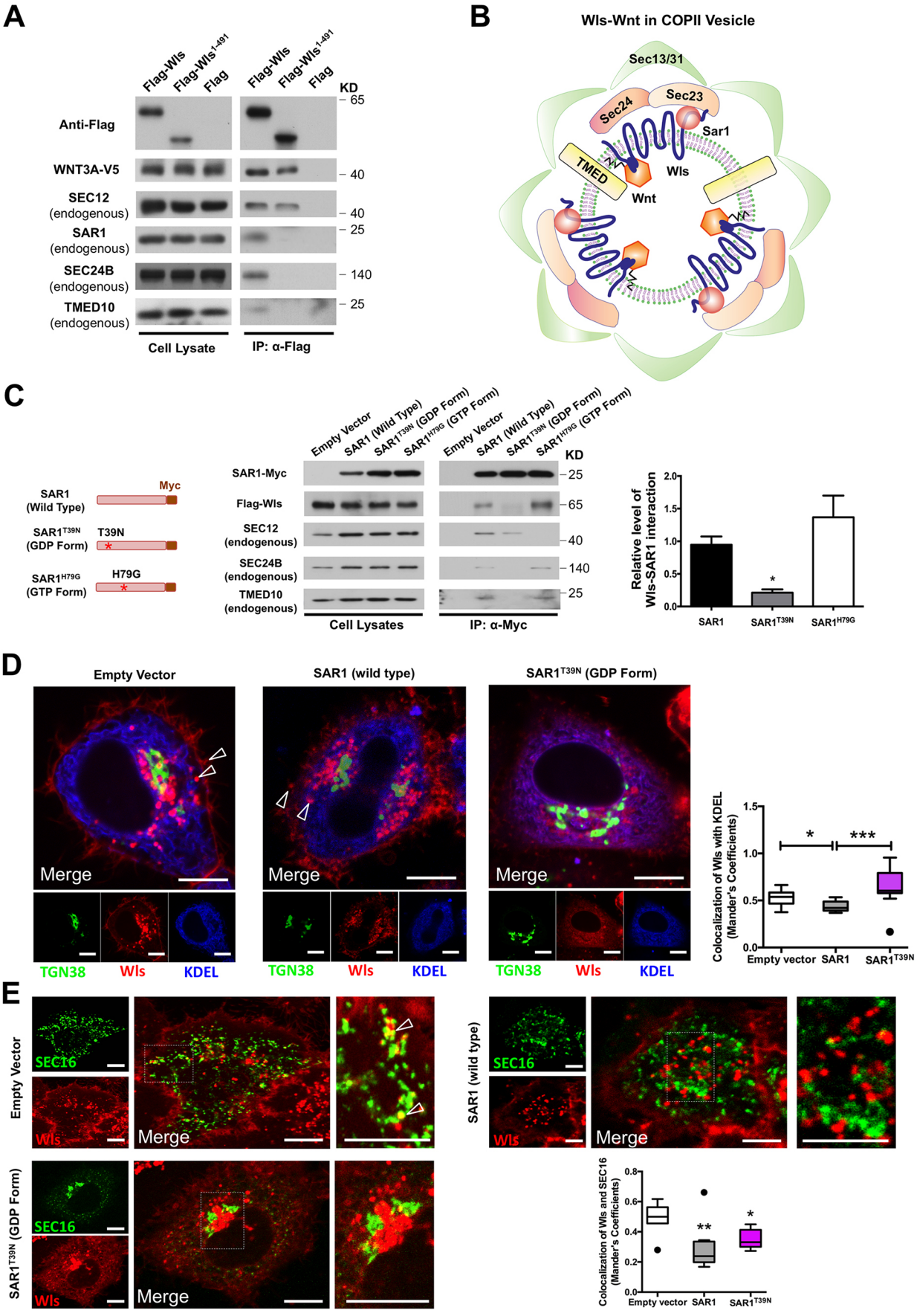

Fig. 1. See next page for legend.

Journal of Cell Science

Journal of Cell Science (2017) 130, 2159-2171 doi:10.1242/jcs.200634

Fig. 1. Wls travels through COPII machinery. (A) Based on proteomic results, co-IP assays were performed on HeLa cells stably expressing 3×Flag, 3×Flag–Wls or 3×Flag–Wls$^{1-491}$. Wnt3a–V5 and endogenous SEC12 showed interaction with Flag–Wls and Flag–Wls$^{1-491}$, while SAR1, SEC24B and TMED10 showed interaction with Flag–Wls but not with Flag-Wls$^{1-491}$ or Flag alone. Data represent more than six independent experiments. (B) A schematic diagram showing a hypothetical COPII vesicle for Wls–Wnt export. (C) Co-IP of Myc-tagged wild-type or mutant SAR1 (T39N and H79G) showed that Wls association was reduced for the SAR1^{T39N} (GDP restricted) compared with that found for wild-type full-length SAR1. Data were quantified (mean±s.e.m.) from two independent experiments each with two duplicates of western blots. Owing to the small size of the Flag peptides, they are not visualized with anti-Flag antibodies in the Flag-only samples. (D) Live-cell images of control (empty vector, *n*=23), SAR1-overexpressing (*n*=9), and SAR1^{T39N}-overexpressing (*n*=16) mCherry–Wls (red) HeLa cells transiently transfected E2-Crimson-KDEL (blue, marking ER) and TGN38–GFP (green, marking Golgi), showing that SAR1^{T39N} impaired the vesicular pattern of wild-type Wls. Arrowheads point to a peripheral vesicle and plasma membrane localization. Tukey box-and-whisker plot illustrating colocalization values, as determined by calculating Manders' coefficients, with outliers shown as dots. **P*<0.05. (E) Live-cell images of control (empty vector, *n*=8), SAR1-overexpressing (*n*=9) or SAR1^{T39N}-expressing (*n*=12) mCherry–Wls (red) HeLa cells transiently transfected with EGFP–SEC16 (green, to mark ER exit sites) showing that SAR1^{T39N} altered the wild-type Wls vesicular pattern at exit sites. Arrowheads point to Wls at exit sites in HeLa cells. Scale bars: 5 µm. **P*<0.05; ***P*<0.01; ****P*<0.001.

and outer (SEC13–SEC31) coats of COPII vesicle that encapsulates the cargo (Aridor et al., 1998). Upon the proper formation of pre-budding COPII complex, SEC13–SEC31 stimulates the GTPase-activating protein (GAP) activities of SEC23 toward SAR1 (Bi et al., 2007; Sato and Nakano, 2005; Yoshihisa et al., 1993). GTP hydrolysis of SAR1 results in the detachment of COPII vesicles from ER membrane (Sato and Nakano, 2005). To examine whether Wls indeed travels through COPII vesicles for ER exit, we immuno-isolated the COPII pre-budding complex by precipitating an overexpressed mutant SAR1^{H79G} that was locked in GTP-restricted form (Aridor et al., 1995). Wls was abundantly detected in isolated SAR1^{H79G} complexes. In contrast, almost no Wls was detected in immunoprecipitates of the GDP-restricted SAR1 mutant SAR1^{T39N}, demonstrating that this mutant did not have the capability to attach to ER membrane (Fig. 1C) (Bielli et al., 2005). Wild-type SAR1 and SAR1^{H79G}, but not Sar1^{T39N}, recruited coat (SEC24B) and adaptor (TMED10) proteins (Fig. 1C), consistent with the notion that active SAR1 stimulates COPII complex assembly. In addition, we detected association of SEC12 with wild-type SAR1 and SAR1^{T39N}, but not SAR1^{H79G} (Fig. 1C). These results were in agreement with the fact that SEC12 has high affinity towards GDP-bound SAR1 (Barlowe and Schekman, 1993).

As SAR1^{T39N} binds to SEC12 but cannot be activated, we hypothesized that SAR1^{T39N} might interfere with SEC12 and prevent Wls from trafficking into COPII vesicles. We imaged live HeLa cells expressing an mCherry-tagged Wls. Overexpression of SAR1^{T39N}, but not wild-type SAR1, indeed impaired the vesicular pattern of Wls (red in Fig. 1D), compared to cells transfected with empty vector. The Golgi, marked by TGN38 (also known as TGOLN2), was intact in SAR1^{T39N} cells (green in Fig. 1D), suggesting that the blockage of Wls trafficking by SAR1^{T39N} was not due to impairment of the Golgi compartment, but potentially occurred at the level of the ER (P<0.05, based on colocalization of Wls and KDEL; Fig. 1D). A GFP-tagged SEC16 has previously been used to label ER exit sites (Bhattacharyya and Glick, 2007). In mCherry–Wls-expressing live cells, we observed a small pool (~3.2%) of total Wls proteins localized adjacent to SEC16-marked exit sites (arrowheads in Fig. 1E). This reflected rapid ER exit dynamics, determined to be on the scale of seconds (Wilhelmi et al., 2016; Antonny et al., 2001; Forster et al., 2006; Sato and Nakano, 2005). There was also a small fraction of SEC16 (14%) adjacent to mature COPII structures (Hughes et al., 2009). Interestingly, overexpressing SAR1^{T39N} led to the dispersion of Wls throughout the cells and away from SEC16-positive exit sites. Of note, large SEC16-positive puncta appeared in SAR1^{T39N}-expressing cells with Wls proteins aggregated near these SEC16 puncta, a phenomenon previously associated with disrupted SAR1 activities (Watson et al., 2006). Overexpression of wild-type SAR1 again did not alter the Wls vesicular pattern, but appeared to promote Wls leaving the exit sites. Thus, alteration of SAR1 activities influenced Wls vesicular distribution.

Recruitment of SAR1 by SEC12 promotes the association of Wls with the COPII complex

As SEC12 is a specific GEF activator for SAR1, we asked whether the Wls–SAR1 association depended on Wls–SEC12 complex formation. We first silenced endogenous SEC12 with a smart-pool of siRNAs in HeLa cells stably expressing Flag–Wls. Compared to what was seen in cells treated with the scrambled control siRNA, knockdown of SEC12 by ~43% led to proportional reductions in Wls–SAR1 (by 55%) and Wls–SEC12 (by 58%) association (Fig. 2A). In contrast, silencing SAR1 by 80% only reduced the level of Wls–SAR1 association, but slightly enhanced Wls–SEC12 association by 12% (Fig. 2A), suggesting that the Wls–SAR1 association depended on SEC12 whereas Wls–SEC12 association was not affected by SAR1.

To test whether Wls–SEC12 complex formation might increase SAR1 recruitment to the Wls complex on ER, we transiently expressed a 6×Myc-tagged SEC12 into HeLa cells that stably expressed wild-type Wls. Both the endogenous SEC12 (black arrowhead, Fig. 2B) and the transfected 6×Myc–SEC12 (white arrowhead, Fig. 2B) co-immunoprecipitated with Wls. This forced Sec12 overexpression increased the level of Wls–SAR1 association by 4-fold (normalized against Wls, Fig. 2B), suggesting that increased Wls–SEC12 complex formation can promote Wls–SAR1 association.

Wls–SAR1 association is dependent on the structural integrity of the Wls C-terminus

As Wls$^{1-491}$, which lacks the entire C-terminal cytosolic tail, failed to enter COPII compartments (Fig. 1A), we then assessed the potential contribution of the Wls C-terminal motif for its association with SEC12 and SAR1. We established additional stable cell lines expressing various Flag-tagged Wls truncated proteins that retained (Wls$^{1-497}$) or lacked (Wls$^{\Delta492-497}$) a conserved hexapeptide motif (Fig. 2C). We found that only full-length Wls, and none of the C-terminally truncated proteins, associated with SAR1. In contrast, all truncated Wls continued to strongly bind to SEC12 (Fig. 2D). Live-cell imaging showed that, unlike the vesicular distributions exhibited by wild-type Wls, Wls$^{\Delta492-497}$ and Wls$^{1-491}$ showed severe ER retention (ER marked by GFP-tagged KDEL; Fig. 2E,F) (Dayel et al., 1999). Interestingly, Wls$^{1-497}$, which retains the hexapeptide motif, showed some vesicular trafficking (arrows in Fig. 2F). Unlike wild-type Wls, Wls$^{\Delta492-497}$ failed to travel to plasma membrane (Fig. 2G), consistent with its failure to bind to any tested COPII components or adaptor proteins (SAR1 in Fig. 2D; SEC24 and TMED10 in Fig. S1). These data suggest that Wls–SAR1 association is highly dependent on the integrity and conformation of C-terminal tail of Wls, misfolding of which might disrupt its communication with COPII machinery, thereby retaining the transporter in ER.

Journal of Cell Science (2017) 130, 2159-2171 doi:10.1242/jcs.200634

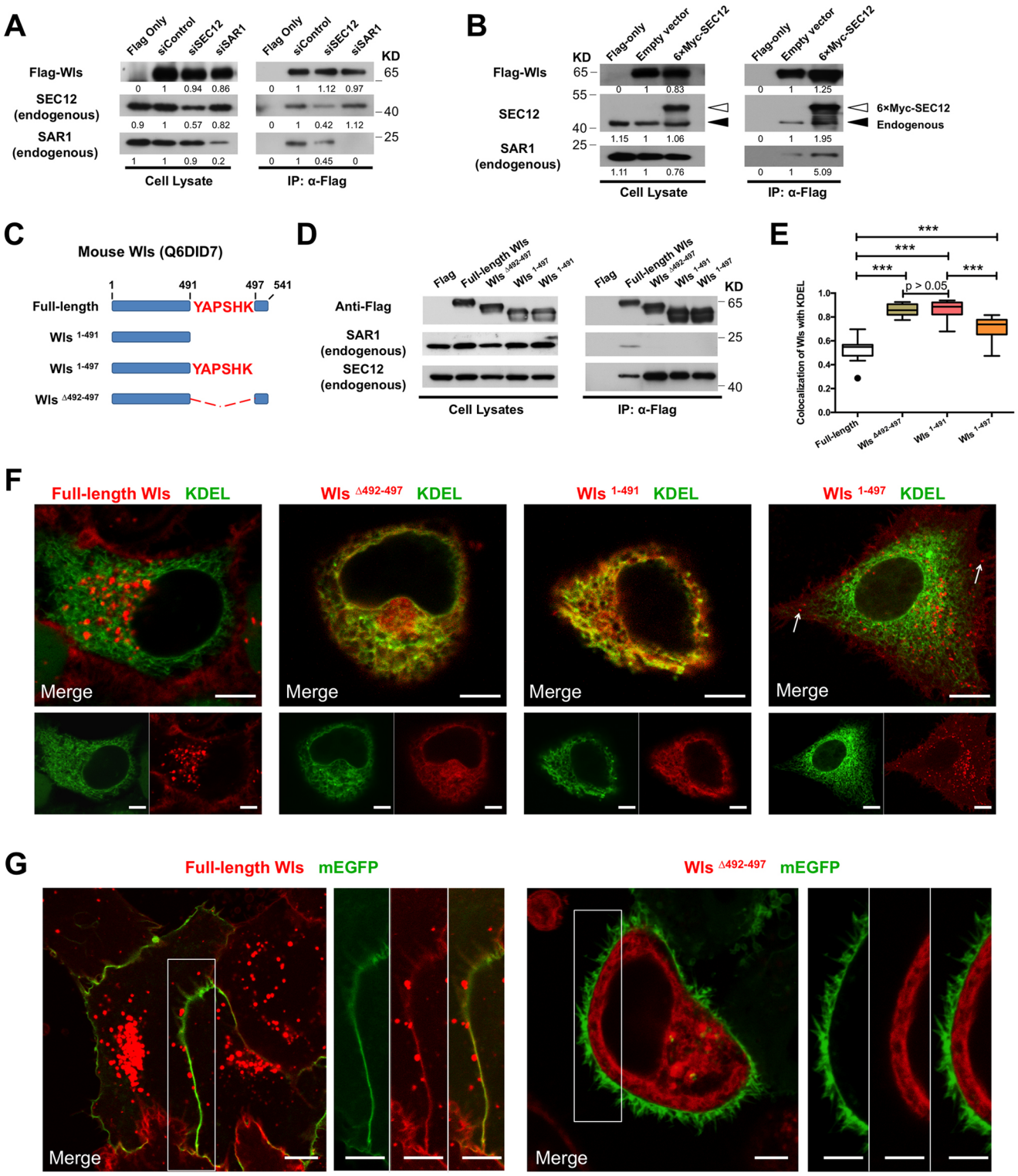

Fig. 2. Wls–SAR1 association depends on SEC12 and an intact Wls C-terminus. (A) Co-IP assays using SEC12-knockdown (siSEC12) or SAR1-knockdown (siSAR1) HeLa cells (stably expressing Flag–Wls) showing that SEC12 knockdown affected Wls–SAR1 association; however, SAR1 depletion did not affect Wls–SEC12 association. Data represent two independent experiments. (B) Co-IP assays showed that overexpression of a 6×Myc–SEC12 construct promoted Wls–SAR1 association. White and black arrowheads point to 6×Myc-SEC12 and the endogenous SEC12, respectively. Data represent two independent experiments. (C) Schematic diagrams showing full-length and various C-terminally truncated Wls proteins: $Wls^{1\text{-}491}$, $Wls^{\Delta 492\text{-}497}$ and $Wls^{1\text{-}497}$. (D) Co-IP assays using stable HeLa cell lines expressing Flag-tagged wild-type or truncated Wls showing that only wild-type Wls associated with endogenous SAR1, while all truncated Wls associated with SEC12. Data represent more than three independent experiments. Owing to the small size of the Flag peptides, they are not visualized with anti-Flag antibodies in the Flag-only samples. (E,F) Live-cell confocal fluorescent images of the subcellular localization of mCherry-tagged wild-type (n=23) and C-terminally truncated Wls proteins (n=19, 27 and 26 for $Wls^{\Delta 492\text{-}497}$, $Wls^{1\text{-}491}$ and $Wls^{1\text{-}497}$, respectively). ER was labeled by EGFP–KDEL. Arrows highlight to peripheral vesicles. (G) $Wls^{\Delta 492\text{-}497}$, which lacks the hexapeptide motif showed ER retention and failed to travel to the plasma membrane. The plasma membrane is highlighted by mEGFP (green). Scale bars: 5 µm. ***P<0.001.

Journal of Cell Science (2017) 130, 2159-2171 doi:10.1242/jcs.200634

Wls–SEC12 interaction is mediated by specific motifs, namely Wls$^{377-431}$ and SEC12$^{301-388}$

The above results suggested a relatively stable and constant complex formation between Wls and SEC12, even when the truncated Wls was retained in the ER (Fig. 2D,F). Importantly, a previously reported antibody against endogenous Wls (Coombs et al., 2010; Yu et al., 2014a) was able to co-immunoprecipitate SEC12 with Wls in HeLa cell lysates (Fig. 3A). In order to systematically map out the responsible motif(s) that mediated Wls–SEC12 interaction, we tested, in co-IP experiments, five additional Flag-tagged Wls truncates with various deletions in predicted transmembrane loop (Wls$^{\Delta 101-232}$, Wls$^{\Delta 233-301}$ or Wls$^{\Delta 302-376}$) or with further truncations in C-terminus (Wls$^{1-376}$, Wls$^{1-431}$) (Fig. 3B,C). Both Wls$^{\Delta 302-376}$ and Wls$^{1-431}$ were able to bind to SEC12; however, Wls$^{1-376}$ failed to bind (red asterisk, Fig. 3C), suggesting that the SEC12-interacting motif resides between amino acids 377 and 431, a fragment predicted to contain a transmembrane (TM) domain and a cytoplasmic loop (Fig. 3B,C). Of note, Wls$^{\Delta 101-232}$, which lacked the Wnt-binding domain (WBD), retained its SEC12 association, but at a lower level (black asterisk, Fig. 3C). In terms of SAR1, only the full-length Wls, and none of the truncated Wls, associated with SAR1 (Fig. 3C). Neither Wls$^{1-431}$ nor Wls$^{1-376}$ were present in vesicles, as judged from confocal images (Fig. S2), indicating that probably only the full-length Wls has the correct conformation acceptable by the COPII ER-exiting machinery.

We performed reciprocal mapping for the Wls-interacting domain in SEC12 using a similar strategy. SEC12 is a single-pass type-II ER TM protein of 417 amino acids. Seven tryptophan-aspartic acid (WD) 40 motifs (Neer et al., 1994) are found at the cytosolic portion of SEC12 (Chardin and Callebaut, 2002). As these WD motifs are always used as scaffolding sites for protein–protein interaction (Stirnimann et al., 2010), we generated five different Myc-tagged truncates (SEC12$^{80-417}$, SEC12$^{80-408}$, SEC12$^{201-408}$, SEC12$^{301-417}$ and SEC12$^{80-388}$) according to the distribution of the WD motifs (Fig. 3D). Truncated SEC12 proteins represented various deletions in the putative N-terminal GEF domain (McMahon et al., 2012), cytosolic regions, TM domain and the ER lumen-residing C-terminal tail. Surprisingly, neither the GEF domain (amino acids 1–79) nor the ER luminal domain (amino acids 408–417) was required for Wls interaction (Fig. 3D,E). A truncated SEC12 (amino acids 201–408) containing only a partial cytosolic region plus the TM domain was sufficient to bind Wls (Fig. 3D,E). Deletion of the TM domain only weakened but did not abolish Wls interaction (see SEC12$^{80-388}$, Fig. 3E), suggesting that the cytosolic domain corresponding to amino acids 301–388 might be responsible for Wls binding.

However, owing to the weakened Wls binding upon removal of the TM domain, it was not clear whether the TM domain also contributed to the interaction. We then generated two chimeric SEC12 proteins: one (EGFP–SEC12$^{389-417}$) with the entire cytosolic portion replaced by an EGFP while preserving the TM and ER luminal domains, and the other (SEC12$^{301-388}$–VAPA™) with the suspected Wls-interacting cytosolic motif (amino acids 301–388) fused to the TM domain of vesicle-associated protein A (VAPA) (Skehel et al., 2000), an unrelated type II ER membrane protein (Fig. 3D). Flag–Wls bound to SEC12$^{301-388}$–VAPA™, but not EGFP–SEC12$^{389-417}$ (Fig. 3E). Finally, Wls$^{1-431}$ was able to bind SEC12$^{301-417}$ but not EGFP–SEC12$^{389-417}$ (Fig. 3F), suggesting that amino acids 301–388 of SEC12 are sufficient to mediate Wls–SEC12 interaction (red box, Fig. 3D).

Wls–SEC12 complex is critical for Wnt secretion

We next assessed the impact of SEC12 on Wnt secretion by using a luciferase assay that monitored the amount of secreted Wnt3a–Gluc (Gluc is *Gaussia* luciferase) in culture medium (Chen et al., 2009; Das et al., 2015). Transient overexpression of wild-type SEC12 enhanced Wnt3a–Gluc secretion by 40% while knocking down SEC12 by 40% was sufficient to decrease Wnt secretion by 24% (Fig. 4A). Likewise, overexpression of SEC12 truncates lacking the GEF domain but capable of Wls-binding inhibited secretion by 62–74%. These inhibitory effects of truncated SEC12 were corroborated by an increased ER retention of endogenous WLS illustrated by it colocalizing with calnexin staining (Fig. 4B–F). As overexpression of SEC12 fragments might alter the global ER exit processes, we further performed Wnt3a–Gluc secretion rescue experiments in Wls-deficient MEFs, which are defective in Wnt secretion (Fig. 4F) (Das et al., 2015). Transient transfection of a full-length Wls (untagged or Flag tagged) into these Wls-deficient MEFs significantly increased the amount of Wnt3a–Gluc that was secreted into the medium (Fig. 4G), an effect not mimicked by the SEC12-binding deficient Wls$^{1-376}$ (Figs 3B,C,4H). The rescuing effect of Wls was specific for Wnt3a–Gluc, but not for Shh–Renilla or Met–Luc (Fig. S3), whose secretions were not dependent on Wls. Note that the observed enhancement of Wnt secretion by transiently transfected Wls was obtained on an ∼8% transfection efficiency. These data suggested that influencing Wls–SEC12 complex formation might affect Wnt secretion.

Wls–SEC12 complex responds to mature Wnt binding to Wls in the ER

Newly synthesized Wnts bind Wls in ER for exocytosis (Yu et al., 2014a). We speculated that the communication between Wls and the SEC12 and COPII machinery might be used to control export of mature Wnts. To determine whether Wls–Wnt binding in ER might influence Wls–SEC12 association, we first transfected differing amounts of V5-tagged Wnt3a into Flag–Wls-expressing HeLa cells, and assessed the effects of the ligand on the association Wls with SEC12 and SAR1. Compared to the basal level of Wls–SEC12 association in cells transfected with empty vector, a pronounced increase of Wls–SEC12 association was found in Wnt3a-transfected cells (Fig. 5A). The level of Wls–SAR1 association was also increased, but to a lesser extent, by Wnt3a overexpression. However, Wnt3a transfection did not increase SEC12 association with Wls $^{\Delta WBD}$, which lacks the Wnt-binding motif (Fig. 5B). These data suggest that an elevated Wnt synthesis and binding to Wls in ER can enhance association of Wls and COPII machinery.

As Wls transports Wnt molecules that are palmitoylated by Porcn in ER (Herr and Basler, 2012), we used the Porcn inhibitor C59 to abolish Wnt lipidation (Proffitt et al., 2013) and Wnt secretion (Fig. 4F). C59 treatment drastically reduced Wls– Wnt3a interaction at 10 nM, which also diminished Wls–SAR1 association (Fig. 5C). Reduction of Wls–SEC12 interaction was only observed at a higher C59 concentration (50 nM) (Fig. 5C), suggesting that the Wls–SEC12 complex was fairly stable in the event of Wnt–Wls dissociation. Importantly, Wls–SEC12 binding remained readily detectable even at 50 nM C59 when Wls–Wnt3a interaction was completely abolished (Fig. 5C). These data suggest that there is a basal level of complex formation between SEC12 and Wls that is not bound to ligand (free) on the ER membrane.

The disruption of Wls–SAR1 association by C59 (Fig. 5C) was corroborated by an observed impairment of the Wls vesicular pattern in live cells (middle panel, Fig. 5D). Likewise, despite its

Journal of Cell Science

Journal of Cell Science (2017) 130, 2159-2171 doi:10.1242/jcs.200634

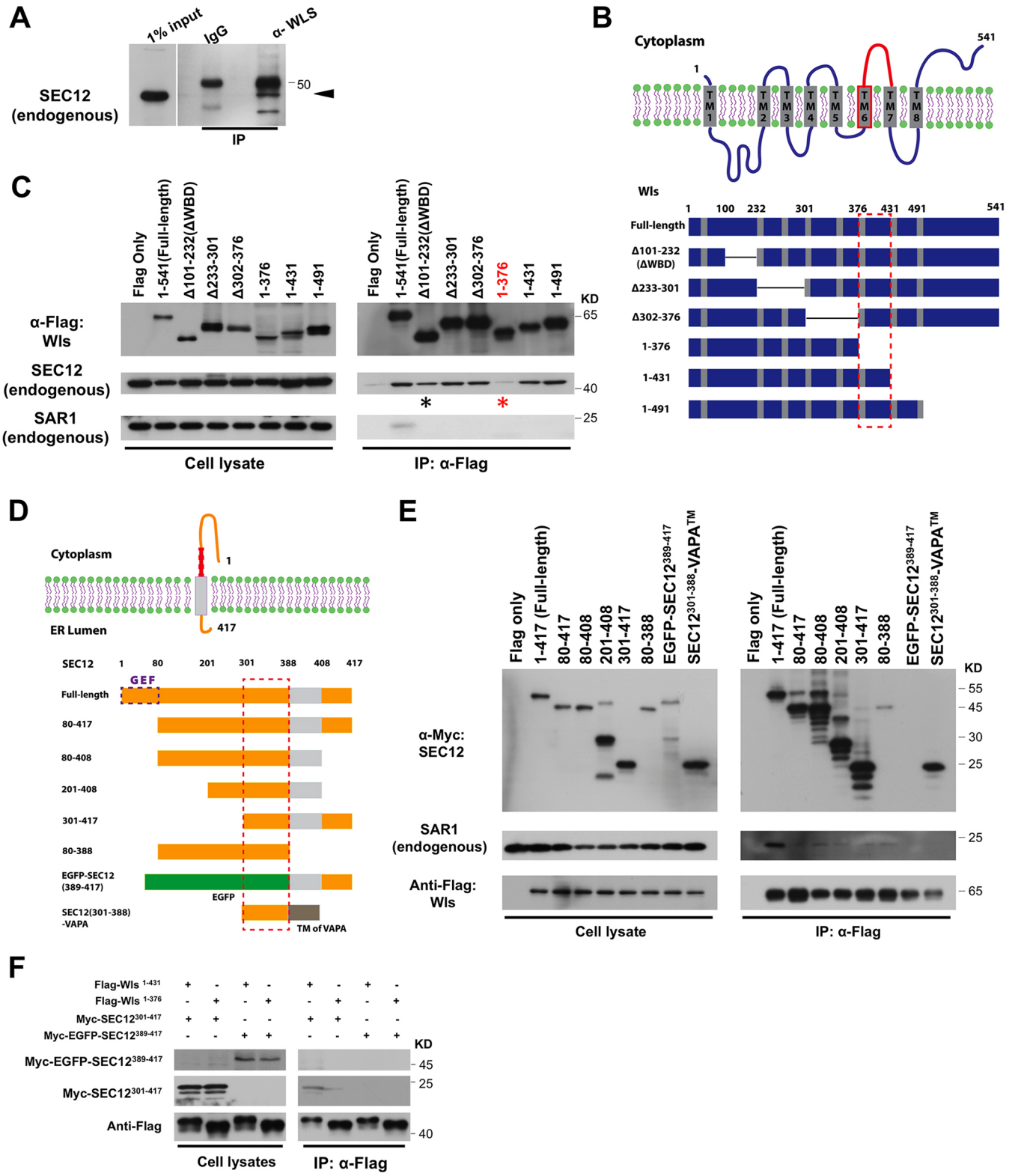

Fig. 3. Wls-SEC12 interaction is mediated by specific protein domains. (A) SEC12 co-immunoprecipitated with WLS in HeLa lysates when using an antibody against endogenous WLS. The arrowhead points to endogenous SEC12. (B,C) SEC12-interacting protein domain mapping in Wls was carried out by performing co-IP analyses (with anti-Flag antibody) with various Flag-tagged truncated Wls proteins as illustrated in diagram. The red asterisk denotes the lost interaction between Wls^{1-376} and SEC12. The red box illustrates the SEC12-interacting motif (amino acids 377–431) in a predicted cytosolic loop of Wls. Note that $Wls^{\Delta 101-232}$ lacking its WBD showed a reduced SEC12 binding (black asterisk). (D,E) A similar strategy to that in B,C for mapping Wls-interacting domains in SEC12 identified a cytosolic motif (amino acids 301-388) that is responsible for Wls association. Note that a chimeric protein ($SEC12^{301-388}$–$VAPA^{TM}$) carrying this motif fused to an independent ER TM domain (from VAPA) showed association with Wls. Owing to the small size of the Flag peptides, they are not visualized with anti-Flag antibodies in the Flag-only samples. (F) Co-IP assay showing that Wls^{1-431} was sufficient to bind $SEC12^{301-417}$. Two or more independent experiments were performed for each co-IP assay.

Journal of Cell Science

Journal of Cell Science (2017) 130, 2159-2171 doi:10.1242/jcs.200634

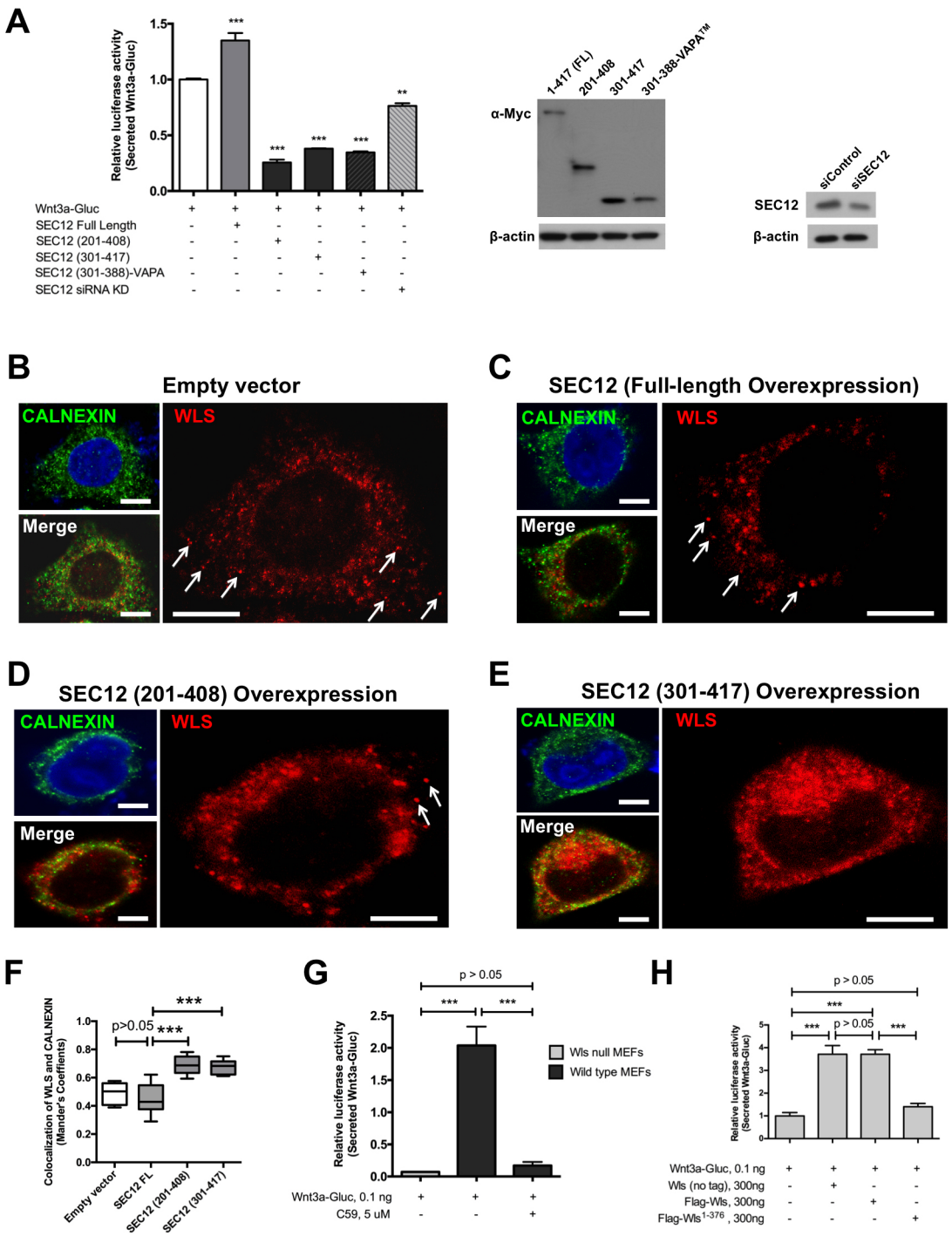

Fig. 4. The SEC12–Wls complex modulates Wnt secretion. (A) HEK293T cells were co-transfected with Wnt3a–Gluc and firefly luciferase, along with wild-type or truncated SEC12 or SEC12-specific siRNA. Luciferase activities were measured from culture media simultaneously harvested 4 h after a change into fresh medium. Data represent mean±s.e.m. for two independent experiments, each with three replicates. The corresponding lysates were blotted for overexpressed or depleted SEC12 proteins (right panels). (B–E) HeLa cells were transfected with empty vector (n=6), full-length SEC12 (n=7) or truncated Myc–SEC12 (n=7 and 9 for $SEC12^{201\text{-}408}$ and $SEC12^{301\text{-}417}$), then fixed and co-stained for endogenous WLS (red) and calnexin (green). Arrows point to peripheral vesicles. (F) Colocalization, as determined by calculating Manders' coefficients, showed a significant increase of WLS–calnexin association in cells transfected with truncated SEC12. Results are presented as a Tukey box-and-whisker plot. (G) A Wnt3a–Gluc assay revealed a severe Wnt secretion defect in Wls-deficient MEFs compared to what was seen in wild-type MEFs. The secretion by wild-type MEFs was inhibited by C59 treatment. (H) Wnt secretion by Wls-deficient MEFs was increased by transient overexpression of a full-length Wls (non-tagged or Flag-tagged), but not by a SEC12-binding defective $Wls^{1\text{-}376}$. Note that the MEF secretory data were obtained on an ~8% transfection efficiency. The experiment was repeated six times. $^{**}P$<0.01; $^{***}P$<0.001.

SEC12-binding capacity (Fig. 5B), $Wls^{\Delta WBD}$ showed strong ER retention (Fig. 5D). In addition, a palmitoylation-defective $Wnt3a^{S209A}$ (Coombs et al., 2010) showed a weaker binding capacity towards Wls, compared to wild-type Wnt3a (Fig. 5E). When we transfected $Wnt3a^{S209A}$ into cells, we observed a smaller effect on Wls–SEC12 association than we did in cells transfected

Journal of Cell Science (2017) 130, 2159-2171 doi:10.1242/jcs.200634

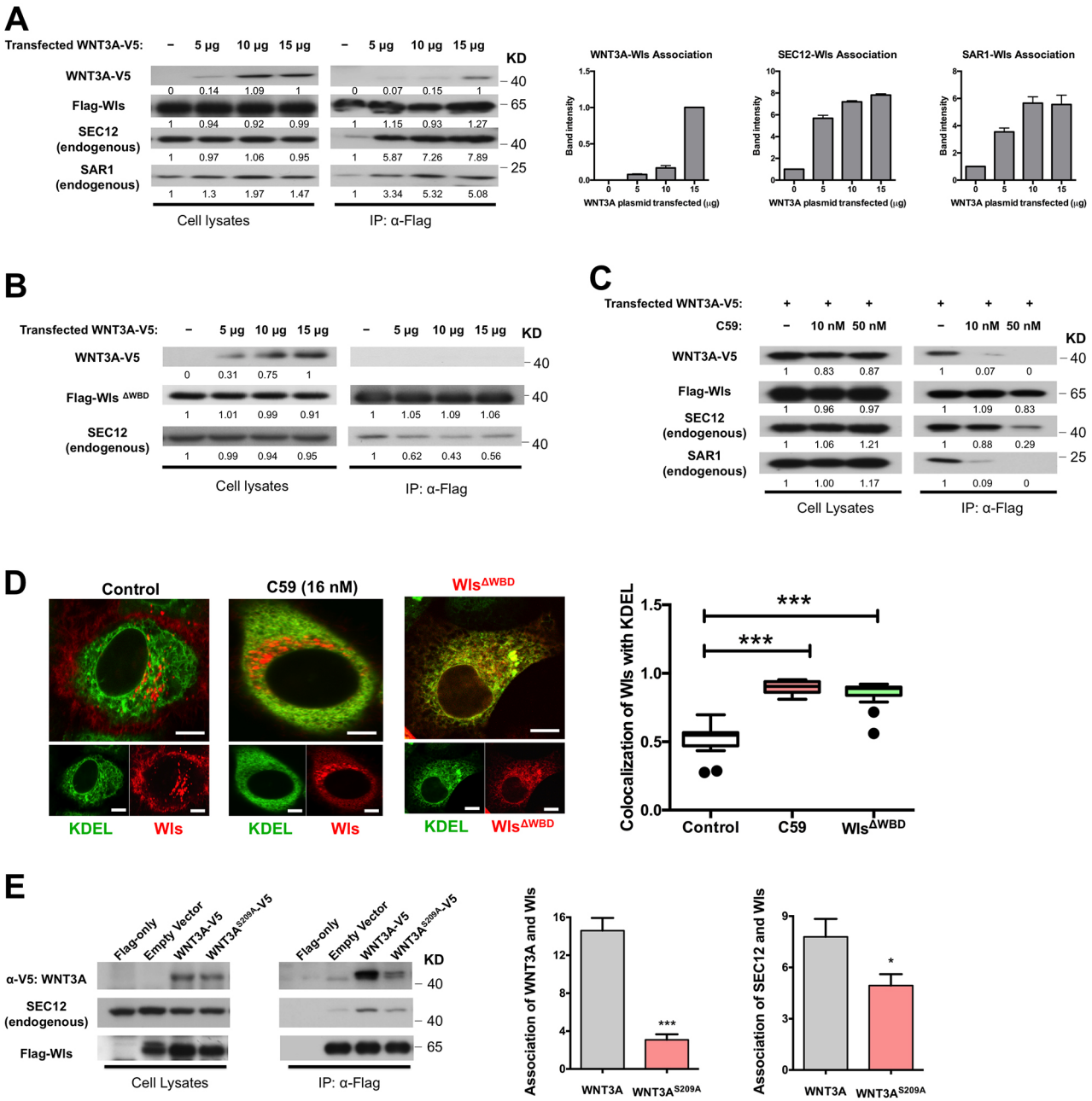

Fig. 5. A pre-formed SEC12-Wls complex is responsive to mature Wnt binding to Wls. (A) Co-IP assays showing that overexpressing Wnt3a–V5 (5, 10 and 15 µg of plasmids) in HeLa cells increased the Wls–SEC12 and Wls–SAR1 associations. (B) Co-IP assays showing that similarly overexpressing Wnt3a–V5 in HeLa cells did not increase SEC12 association with Wls$^{\Delta WBD}$, which lacks a Wnt-binding domain. (C) Co-IP assays showing that treatment of HeLa cells with Porcn inhibitor C59 (10 or 50 nM) diminished the Wls–Wnt3a and Wls–SAR1 associations. Note that 50 nM C59 only reduced, but did not abolish, Wls–SEC12 complex formation. Vehicle (DMSO) was used on cells that were not treated with C59. (D) C59 treatment partially increased ER retention of Wls, while Wls$^{\Delta WBD}$ showed a severe ER-retention pattern. (E) Co-IP assays showing that, compared to wild-type Wnt3a-transfected cells, cells that were transfected with Wnt3a^{S209A} with less Wls-binding capacity also showed less Wls–SEC12 association. Results in D are presented as a Tukey box-and-whisker plot. Three independent experiments were performed for each co-IP assay. Owing to the small size of the Flag peptides, they are not visualized with anti-Flag antibodies in the Flag-only samples. Scale bars: 5 µm. *P<0.05; ***P<0.001.

with wild-type Wnt3a (Fig. 5E). Collectively, these data support a model where binding of mature Wnts to Wls in the ER might relay a signal to the pre-formed Wls–SEC12 complex on the ER membrane to facilitate COPII-mediated Wnt vesicle assembly and export. However, ligand-free Wls, despite its SEC12-binding, has limited access to SAR1 and COPII pre-budding complex, presumably avoiding unnecessary export of Wls that is not bound to ligand.

DISCUSSION

Although different Wnts regulate diverse signaling pathways in ligand-receiving cells, secretion of virtually all vertebrate Wnts share two remarkably similar features: lipid modification by Porcn in ER and utilization of Wls as the transporter to reach the plasma membrane. Cell fractionation studies demonstrated an ER pool of Wls that interacts with Wnt molecules (Yu et al., 2014a). Knocking down Wls in *Drosophila* caused ER stress, a phenotype that was

Journal of Cell Science (2017) 130, 2159-2171 doi:10.1242/jcs.200634

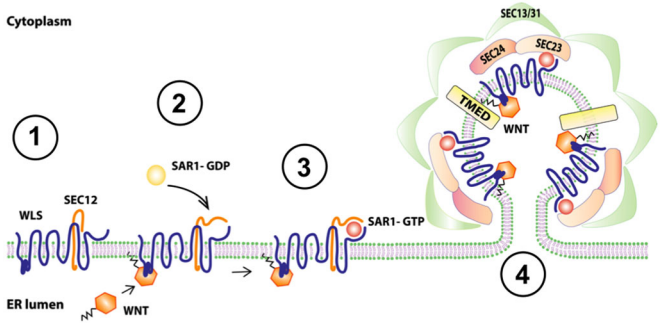

Fig. 6. A schematic diagram illustrating COPII-dependent ER export of Wls–Wnt. (1) There is a basal level of pre-formed Wls–SEC12 complex, which is directly mediated by specific cytosolic motifs, on ER membrane. (2) Upon mature Wnt binding to Wls in the ER, the Wls–SEC12 association is enhanced via an unknown mechanism, resulting in increased recruitment of SAR1 to the Wls–SEC12 complex. The C-terminal tail of Wls appears to be required for this process. (3) SEC12 activates SAR1. (4) GTP-bound SAR1 initiates COPII vesicle assembly at ER exit sites, exporting Wls–Wnt from the ER, while leaving SEC12 in the ER membrane.

also induced by *Porcupine* depletion (Zhang et al., 2016), suggesting that defective Wls or Porcn function blocks Wnt secretion at the level of ER. However, the exact molecular mechanism that regulates the packaging and export of Wnt secretory vesicles from ER has not been fully understood. Our study provided a direct link between ligand-bound Wls and major molecular components of COPII ER-exiting machinery (Fig. 6). We affirmed the importance of binding of mature Wnts to Wls within ER, which may serve as a crucial signal to initiate the assembly of ER-exiting vesicles for Wnt export.

Wnts, after exiting the ER, can reach the cell surface via various routes, such as in exocytic vesicles (Das et al., 2015), exosomes (Gross et al., 2012; Korkut et al., 2009) or through transcytosis (Gallet et al., 2008). Our data pointed to an initial ER-exiting process that is probably common to the secretion of all *de novo* synthesized Wnt proteins. Our proteomic analysis did not detect any ER-to-Golgi intermediate complex proteins that regulate an alternative ER-to-Golgi transport pathway in addition to the COPII machinery. It is noteworthy that in addition to the canonical Wls (splicing variant 1) that is conserved across animal species, an alternative splicing variant 2 (widely expressed in primates) that lacks key motifs for retrograde trafficking (Yu et al., 2014a) still retains the conserved hexapeptide motif described in our study. At this moment, our data does not support an indispensable role for this motif in Wls–SEC12 interaction. It is plausible that this proline-containing motif is critical for Wls to adopt a strict conformation for recognition by the ER export machinery (Fig. 6), as loss of this motif alone disrupts Wls–COPII communication. The truncated transporter $Wls^{1\text{-}497}$, although being incapable of SAR1 binding, gained partial vesicular trafficking ability, suggesting that retaining this hexapeptide provided certain structural cues that are required for ER exit. The precise role of this motif and whether a SAR1-independent Wls export mechanism exists require further investigations.

Wnt and Wls have been individually suggested to undergo retrograde Golgi-to-ER transport in COPI vesicles (Yu et al., 2014a; Zhang et al., 2016). To our knowledge, this study represents the first to define Wls–SEC12 and Wls–COPII interactions. Activated SAR1 initiates the formation of COPII-coated vesicles and triggers the release of the cargo-bearing vesicles from ER. Wls appears to use the same machinery for ER exit as reported for other growth factors, including collagen type I (Jin et al., 2012), type VII (Saito et al., 2009) and the G-protein-coupled receptors, AT1R, β_2-AR, α_{2B}-AR and hCaR (Dong et al., 2008; Zhuang et al., 2010). However, the molecular basis of Wls–COPII communication differs from mechanisms proposed for other cargos. Formation of the Wls–SEC12 complex was detected in cells treated with high concentrations of Porcn inhibitor. Under these conditions, no binding between Wnt3a and Wls was detected, suggesting that there was a basal level of complex formation between Wls that was not bound to ligand (free) and SEC12 on the ER membrane. Increased production of wild-type Wnt ligands in our experiments promoted a substantial Wls–SEC12 association, a change that was not seen with mutant ligands lacking lipidation. Thus, upon receiving a signal of Wls engagement by mature Wnts from the ER lumen, the pre-formed Wls–SEC12 complex may be used as a 'ready-to-go' site for rapid SAR1 docking and activation (Fig. 6). In contrast, the pre-formed complex of collagen type VII and its transporter TANGO1–cTAGE5 (TANGO1 is also known as MIA3) recruits Sec12 to the ER exit site and subsequently triggers packaging of collagen into COPII vesicles (Saito et al., 2014), a mechanism that may not be utilized by Wls. Our data collectively indicate that a pre-formed Wls–SEC12 complex pool can be expanded or stabilized by binding of mature Wnts to Wls, illustrating an unappreciated ligand-dependent ER-exporting mechanism for Wnts. Currently it is not clear how Wnt–Wls binding in the ER influences Wls–SEC12 binding, but a probable alteration of Wls conformation may be induced by ligand engagement, which may stabilize Wls–SEC12 association or expose more SEC12-binding sites. It is noteworthy that on the plasma membrane of Wnt-receiving cells, Wnt-binding to its surface receptors, Frizzled and low-density lipoprotein receptor-related protein 5 and 6 (LRP5/6, a single-pass TM protein), results in a tertiary complex formation (MacDonald et al., 2009), a scenario with some similarities to Wnt–Wls–SEC12 complex at the ER membrane.

In our model, fully modified mature Wnt molecules may be the ultimate drivers for Wls–Wnt export via the COPII machinery. This ER-exiting strategy may ensure economic utilization of Wls for transporting only functional Wnts (Fig. 6). Taken together, our study supports a sophisticated mechanism controlling Wnt ligand entry into the early secretory pathway.

MATERIALS AND METHODS

Cell lines

HeLa and HEK293T cells (ATCC) were grown in Dulbecco's modified Eagle's medium (DMEM) (Corning) supplied with 10% fetal bovine serum (FBS) (GIBCO). Derivation and maintenance of wild-type and Wls-deficient MEFs have been described previously (Das et al., 2015).

Retroviral production and establishment of stable cell lines

GP2-293 cells were grown in a 10-cm dish until 90% confluence and transfected with Flag-, EGFP- or mCherry-tagged wild-type or mutant Wls in a pQCXIP vector backbone with pVSVG using Lipofectamine 3000 (Life Technologies) as described previously (Yu et al., 2014c). At 6 h after transfection, viral harvest medium (DMEM with 10% FBS plus 100 ng/ml BSA) was applied to maximize the retroviral production. After an additional 2 days, the medium containing retroviruses was collected, centrifuged at 1000 ***g*** to remove cell debris and ultracentrifuged at 15,000 ***g*** at 4°C for 2 h. After ultracentrifugation, the supernatant was discarded and the viral pellet was re-suspended with DMEM for HeLa cell infection. HeLa cells at 80% confluence in a 10-cm dish were incubated with the viruses in DMEM for 6 h and cultured in DMEM with 10% FBS for another 24 h. Stable clones were selected by using puromycin (2 µg/ml) for 7 days. The expression of recombinant Wls proteins was assessed by western blotting and live-cell imaging.

Journal of Cell Science (2017) 130, 2159-2171 doi:10.1242/jcs.200634

Plasmids and siRNA

cDNA for mCherry and oligonucleotide sequences for three copies of Flag sequence (DYKDDDDK) were inserted into the NotI/AgeI sites of pQCXIP vector (Clontech) as N-terminal tags, referred to as pQCXIP-mCherry or pQCXIP-3×Flag vectors. Full-length or truncated Wls sequences were amplified from a mouse Wls (UniProtKB Q6DID7) cDNA clone (Fu et al., 2009). cDNA fragments of Wls (1–541, 1–491, 1–497, 1–431 and 1–376), were subcloned into the XhoI/EcoRI sites of the pQCXIP-3×Flag vector, to generate Flag-tagged recombinant fusion constructs. A non-tagged full-length Wls cDNA was cloned into the XhoI/EcoRI sites of pQCXIP expression vector and used in Wnt secretion assay. Site-directed mutagenesis was used to generate mutant constructs, including Wnt3a^{S209A}, Sar1a^{T39N} and Sar1a^{H79G}, following the manufacturer's protocol (New England Biolabs). In order to avoid introducing additional oligonucleotides between fusion proteins, truncated forms of Wls (Δ101–232, Δ233–301, Δ302–376) were created using NEBuilder HiFi DNA assembly methods (New England Biolabs). The human SEC12 cDNA clone (SC319881) and human SAR1A–Myc–Flag cDNA ORF clone (RC201450) were purchased from Origene. SEC12 fragments (1–417, 80–417, 80–408, 201–408, 301–417 and 80–388) were then amplified from the cDNA clone. Using NEBuilder HiFi DNA assembly methods, EGFP–SEC12$^{389-417}$ was generated by inserting cDNA of EGFP between the Myc tag and amino acid 389 of SEC12. SEC12$^{301-388}$–VAPA™ was generated by fusing oligonucleotides encoding the TM region (LPSLLVVIAAIFIGFFLGKFI) of human VAPA after amino acid 388 of SEC12. All SEC12 fragments (1–417, 80–417, 80–408, 201–408, 301–417, 80–388, EGFP-SEC12$^{389–417}$ and SEC12$^{301–388}$-VAPA^{TM}) were cloned into pCS2-6xMyc vector (the Myc tag is EQKLISEEDL) between the EcoRI and Xhol sites. Plasmids pEF.myc.ER-E2-Crimson (#38770) for labeling ER in the far-red channel, pcDNA-WNT3A-V5 (#34927), pmGFP-SEC16A (#15776), pcDNA3-Shh-Renilla (#37677) were purchased from Addgene. The Metridia luciferase (Met-Luc) construct was from Clontech (#631704). pmEGFP was generated by inserting oligonucleotides encoding the first 10 amino acids (MGCVCSSNPE) of mouse LCK into Xho I/EcoR I sites of the pEGFP N1 vector to attach the plasma membrane-targeting motif to EGFP at its N terminus, to label the plasma membrane. Human TGN38-encoding sequences was cloned in frame into pEGFP-N1 vector to generate a C-terminal EGFP-tagged TGN38 plasmid pTGN38-EGFP. pEGFP-KDEL was a gift from Dr. Nihal Altan-Bonnet (National Heart, Lung and Blood Institute, USA). Human PREB (M-017655-00-0020) siGENOME siRNAs SMARTpool and ON Human SAR1A (L-016756-00-0020) TARGETplus SMARTpool were purchased from Dharmacon.

Antibodies

Antibodies were used as follows: V5 HRP (1:2000, R96125 Thermo Fisher); Myc HRP (1:1000, RF236739 Thermo Fisher); mouse polyclonal anti-FLAG (1:20,000, F1804, Sigma), Flag-HRP (1:2000, A8592, Sigma); Sec12 (1:1000, 10146-2-2AP), Sar1a (1:1000, 22291-1-AP), TMED10 (1:1000, 15199-1-AP) from Proteintech; Sec24B (1:1000, 12042S) Calnexin (1:1000, 2433S) from Cell Signaling. HRP-conjugated anti-rabbit-IgG was purchased from GE Healthcare. Anti-FLAG M2 agarose (A2220, Sigma). Anti-FLAG M2 agarose beads were purchased from Sigma and c-Myc monoclonal antibody-agarose beads were from Clontech Inc.

Co-immunoprecipitation and proteomic analysis

Stable and transiently transfected cells were washed once with PBS and then lysed with 600 µl per plate (for a 10 cm plate) of lysis buffer (50 mM Tris-HCl, pH7.4, 150 mM NaCl, 1 mM EDTA, 1× Roche proteinase inhibitor cocktail, and 0.25% Triton X-100). Cells were lysed and sonicated at 4°C. Protein (2 mg) was mixed with 40 µl wet volume of anti-Flag M2 affinity gel (A2220, Sigma) and incubated at 4°C for 6 h. The suspension was pelleted by centrifugation at 1000 ***g*** for 1 min and washed three times with washing buffer (50 mM Tris-HCl pH 7.4 and 150 mM NaCl). Then the bound proteins were eluted with 50 µl 3×Flag peptides (150 ng/µl), mixed with SDS sample buffer (NP0007, Life Technology) and denatured at 95°C for 5 mins, before being analyzed by SDS-PAGE and immunoblotting, as previously described (Yu et al., 2014b). For proteomic analysis of wild-type and trafficking-defective Wls, immunoprecipitations of Flag–Wls or Flag–Wls$^{1-491}$ were performed by using anti-FLAG M2 agarose beads on extracts from HeLa cell lines stably expressing the above proteins. The same amounts of precipitates (n=2 for each of precipitated Flag proteins) were resolved by SDS-PAGE, followed by Ruby protein gel staining. Bands at 50 kDa corresponding to the antibody heavy chains were excised and excluded from the analysis. The remaining lane of gel for each sample was subjected to in-gel digestion and mass spectrometry identifications (Li et al., 2013). For IP of endogenous Wls, the YJ5 antibody (EMD Millipore) was used (Coombs et al., 2010).

Confocal live-cell imaging

The procedure of confocal immunofluorescence was as described previously (Sakamori et al., 2012, 2014). Briefly, HeLa cells were cultured in a glass-bottom chamber (LabTek Corporation, Catalog # 155383) and imaged using a Zeiss LSM510META confocal laser scanning confocal microscope (Carl Zeiss, USA) using high-magnification, high numerical aperture objective (Plan-Apochromat 63×1.4 NA oil DIC). To maintain cell viability, live cells were maintained on the microscope stage in a temperature-, CO_2- and humidity-controlled environmental chamber. C59 {4-(2-Methyl-4-pyridinyl)-N-[4-(3-pyridinyl)phenyl] benzeneacetamide} was purchased from CellagenTech (C7641-2s) and dissolved in DMSO and administrated into culture medium at the indicated concentrations. Cells were treated with the same volumes of DMSO in control groups.

Secretion assay

To measure Wnt3a–Gluc secretory activities, cells were transiently transfected with Wnt3a–Gluc, with firefly luciferase serving as transfection control. At 6 h after transfection, the medium was changed. Supernatant and cell lysates were simultaneously collected after 2–4 h. Measurement of Shh–Renilla and Met–Luc secretion, the dual luciferase assay and data analysis were as described previously (Das et al., 2015).

Quantifications and statistical analysis

All data were analyzed from independent experiments. Co-IP and western blot experiments were repeated two or more times. Bands were quantified by NIH Image J (ver 2.0.0-rc-43/1.51j) with mean values shown with error bars representing s.e.m. (Schneider et al., 2012). To quantify the colocalization between fluorescently labeled Wls, KDEL and SEC16, Manders' coeffieient values were computed from confocal cellular images using the Coloc2 plugin for ImageJ (Fiji) (Schindelin et al., 2012), as previously used for determining colocalization of Sec12–Sec16, Sec12-KDEL and Sec12-cTAGE5 (Saito et al., 2014). To assess the percentage of Wls (red) colocalizing with SEC16 (green), yellow signals were captured through the 'Colocalization Highlighter' plugin and the total pixel numbers corresponding to a signal channel or yellow particles (size equal or above 10 pixels) were obtained using ImageJ (WCIF from http://www.uhnres.utoronto.ca/facilities/wcif/). Data were plotted as a Tukey box-and-whisker plot with outliners shown as dots. Statistical analysis was performed using one-way ANOVA on the basis of experimental setups, and graphs were constructed with GraphPad Prism 5, and is represented as *P<0.05; **P<0.01 and ***P<0.001.

Competing interests

The authors declare no competing or financial interests.

Author contributions

Conceptualization: J.S., S.Y., E.M.B., N.G.; Methodology: J.S., S.Y., X.Z., C.C., O.A., T.D., N.G.; Software: J.S.; Validation: J.S., S.Y., X.Z., O.A., N.G.; Formal analysis: J.S., S.Y., X.Z., E.M.B., N.G.; Investigation: J.S., S.Y., X.Z., C.C., O.A., T.D., E.M.B., N.G.; Resources: N.G.; Data curation: J.S., S.Y., X.Z., C.C., O.A., T.D.; Writing - original draft: J.S., N.G.; Writing - review & editing: J.S., E.M.B., N.G.; Visualization: J.S., S.Y., X.Z., C.C., N.G.; Supervision: N.G.; Project administration: N.G.; Funding acquisition: N.G.

Funding

This work is supported by National Institutes of Health (NIH) grants (DK102934 and CA178599); an Initiative for Multidisciplinary Research Teams (IMRT) award from Rutgers University; the National Science Foundation (NSF)/BIO/IDBR (1353890); and the American Cancer Society [a Research Scholar grant (RSG-15-060-01-TBE) to N.G.], and Crohn's and Colitis Foundation of America career development award (406794) to S.Y. Deposited in PMC for release after 12 months.

Supplementary information

Supplementary information available online at
http://jcs.biologists.org/lookup/doi/10.1242/jcs.200634.supplemental

References

Antonny, B., Madden, D., Hamamoto, S., Orci, L. and Schekman, R. (2001). Dynamics of the COPII coat with GTP and stable analogues. *Nat. Cell Biol.* **3**, 531-537.

Aridor, M., Bannykh, S. I., Rowe, T. and Balch, W. E. (1995). Sequential coupling between COPII and COPI vesicle coats in endoplasmic reticulum to Golgi transport. *J. Cell Biol.* **131**, 875-893.

Aridor, M., Weissman, J., Bannykh, S., Nuoffer, C. and Balch, W. E. (1998). Cargo selection by the COPII budding machinery during export from the ER. *J. Cell Biol.* **141**, 61-70.

Aridor, M., Fish, K. N., Bannykh, S., Weissman, J., Roberts, T. H., Lippincott-Schwartz, J. and Balch, W. E. (2001). The Sar1 GTPase coordinates biosynthetic cargo selection with endoplasmic reticulum export site assembly. *J. Cell Biol.* **152**, 213-229.

Banziger, C., Soldini, D., Schutt, C., Zipperlen, P., Hausmann, G. and Basler, K. (2006). Wntless, a conserved membrane protein dedicated to the secretion of Wnt proteins from signaling cells. *Cell* **125**, 509-522.

Barlowe, C. and Schekman, R. (1993). SEC12 encodes a guanine-nucleotide-exchange factor essential for transport vesicle budding from the ER. *Nature* **365**, 347-349.

Bartscherer, K., Pelte, N., Ingelfinger, D. and Boutros, M. (2006). Secretion of Wnt ligands requires Evi, a conserved transmembrane protein. *Cell* **125**, 523-533.

Belenkaya, T. Y., Wu, Y., Tang, X., Zhou, B., Cheng, L., Sharma, Y. V., Yan, D., Selva, E. M. and Lin, X. (2008). The retromer complex influences Wnt secretion by recycling wntless from endosomes to the trans-Golgi network. *Dev. Cell* **14**, 120-131.

Bhattacharyya, D. and Glick, B. S. (2007). Two mammalian Sec16 homologues have nonredundant functions in endoplasmic reticulum (ER) export and transitional ER organization. *Mol. Biol. Cell* **18**, 839-849.

Bi, X., Mancias, J. D. and Goldberg, J. (2007). Insights into COPII coat nucleation from the structure of Sec23.Sar1 complexed with the active fragment of Sec31. *Dev. Cell* **13**, 635-645.

Bielli, A., Haney, C. J., Gabreski, G., Watkins, S. C., Bannykh, S. I. and Aridor, M. (2005). Regulation of Sar1 NH2 terminus by GTP binding and hydrolysis promotes membrane deformation to control COPII vesicle fission. *J. Cell Biol.* **171**, 919-924.

Buechling, T., Chaudhary, V., Spirohn, K., Weiss, M. and Boutros, M. (2011). p24 proteins are required for secretion of Wnt ligands. *EMBO Rep.* **12**, 1265-1272.

Chardin, P. and Callebaut, I. (2002). The yeast Sar exchange factor Sec12, and its higher organism orthologs, fold as beta-propellers. *FEBS Lett.* **525**, 171-173.

Chen, B., Dodge, M. E., Tang, W., Lu, J., Ma, Z., Fan, C.-W., Wei, S., Hao, W., Kilgore, J., Williams, N. S. et al. (2009). Small molecule-mediated disruption of Wnt-dependent signaling in tissue regeneration and cancer. *Nat. Chem. Biol.* **5**, 100-107.

Clevers, H. and Nusse, R. (2012). Wnt/beta-catenin signaling and disease. *Cell* **149**, 1192-1205.

Coombs, G. S., Yu, J., Canning, C. A., Veltri, C. A., Covey, T. M., Cheong, J. K., Utomo, V., Banerjee, N., Zhang, Z. H., Jadulco, R. C. et al. (2010). WLS-dependent secretion of WNT3A requires Ser209 acylation and vacuolar acidification. *J. Cell Sci.* **123**, 3357-3367.

Das, S., Yu, S., Sakamori, R., Stypulkowski, E. and Gao, N. (2012). Wntless in Wnt secretion: molecular, cellular and genetic aspects. *Front. Biol.* **7**, 587-593.

Das, S., Yu, S., Sakamori, R., Vedula, P., Feng, Q., Flores, J., Hoffman, A., Fu, J., Stypulkowski, E., Rodriguez, A. et al. (2015). Rab8a vesicles regulate Wnt ligand delivery and Paneth cell maturation at the intestinal stem cell niche. *Development* **142**, 2147-2162.

Dayel, M. J., Hom, E. F. Y. and Verkman, A. S. (1999). Diffusion of green fluorescent protein in the aqueous-phase lumen of endoplasmic reticulum. *Biophys. J.* **76**, 2843-2851.

Dong, C., Zhou, F., Fugetta, E. K., Filipeanu, C. M. and Wu, G. (2008). Endoplasmic reticulum export of adrenergic and angiotensin II receptors is differentially regulated by Sar1 GTPase. *Cell. Signal.* **20**, 1035-1043.

Duraiswamy, A. J., Lee, M. A., Madan, B., Ang, S. H., Tan, E. S. W., Cheong, W. W. V., Ke, Z., Pendharkar, V., Ding, L. J., Chew, Y. S. et al. (2015). Discovery and Optimization of a Porcupine Inhibitor. *J. Med. Chem.* **58**, 5889-5899.

Feng, Q. and Gao, N. (2015). Keeping Wnt signalosome in check by vesicular traffic. *J. Cell. Physiol.* **230**, 1170-1180.

Forster, R., Weiss, M., Zimmermann, T., Reynaud, E. G., Verissimo, F., Stephens, D. J. and Pepperkok, R. (2006). Secretory cargo regulates the turnover of COPII subunits at single ER exit sites. *Curr. Biol.* **16**, 173-179.

Franch-Marro, X., Wendler, F., Guidato, S., Griffith, J., Baena-Lopez, A., Itasaki, N., Maurice, M. M. and Vincent, J.-P. (2008). Wingless secretion requires endosome-to-Golgi retrieval of Wntless/Evi/Sprinter by the retromer complex. *Nat. Cell Biol.* **10**, 170-177.

Fu, J., Jiang, M., Mirando, A. J., Yu, H.-M. and Hsu, W. (2009). Reciprocal regulation of Wnt and Gpr177/mouse Wntless is required for embryonic axis formation. *Proc. Natl. Acad. Sci. USA* **106**, 18598-18603.

Gallet, A., Staccini-Lavenant, L. and Thérond, P. P. (2008). Cellular trafficking of the glypican Dally-like is required for full-strength Hedgehog signaling and wingless transcytosis. *Dev. Cell* **14**, 712-725.

Gao, X. and Hannoush, R. N. (2014). Single-cell imaging of Wnt palmitoylation by the acyltransferase porcupine. *Nat. Chem. Biol.* **10**, 61-68.

Gasnereau, I., Herr, P., Chia, P. Z. C., Basler, K. and Gleeson, P. A. (2011). Identification of an endocytosis motif in an intracellular loop of Wntless protein, essential for its recycling and the control of Wnt protein signaling. *J. Biol. Chem.* **286**, 43324-43333.

Goodman, R. M., Thombre, S., Firtina, Z., Gray, D., Betts, D., Roebuck, J., Spana, E. P. and Selva, E. M. (2006). Sprinter: a novel transmembrane protein required for Wg secretion and signaling. *Development* **133**, 4901-4911.

Gross, J. C., Chaudhary, V., Bartscherer, K. and Boutros, M. (2012). Active Wnt proteins are secreted on exosomes. *Nat. Cell Biol.* **14**, 1036-1045.

Harterink, M., Port, F., Lorenowicz, M. J., McGough, I. J., Silhankova, M., Betist, M. C., van Weering, J. R. T., van Heesbeen, R. G. H., Middelkoop, T. C., Basler, K. et al. (2011). A SNX3-dependent retromer pathway mediates retrograde transport of the Wnt sorting receptor Wntless and is required for Wnt secretion. *Nat. Cell Biol.* **13**, 914-923.

Herr, P. and Basler, K. (2012). Porcupine-mediated lipidation is required for Wnt recognition by Wls. *Dev. Biol.* **361**, 392-402.

Herr, P., Hausmann, G. and Basler, K. (2012). WNT secretion and signalling in human disease. *Trends Mol. Med.* **18**, 483-493.

Hughes, H., Budnik, A., Schmidt, K., Palmer, K. J., Mantell, J., Noakes, C., Johnson, A., Carter, D. A., Verkade, P., Watson, P. et al. (2009). Organisation of human ER-exit sites: requirements for the localisation of Sec16 to transitional ER. *J. Cell Sci.* **122**, 2924-2934.

Janda, C. Y., Waghray, D., Levin, A. M., Thomas, C. and Garcia, K. C. (2012). Structural basis of Wnt recognition by Frizzled. *Science* **337**, 59-64.

Jin, J., Kittanakom, S., Wong, V., Reyes, B. A. S., Van Bockstaele, E. J., Stagljar, I., Berrettini, W. and Levenson, R. (2010). Interaction of the mu-opioid receptor with GPR177 (Wntless) inhibits Wnt secretion: potential implications for opioid dependence. *BMC Neurosci.* **11**, 33.

Jin, L., Pahuja, K. B., Wickliffe, K. E., Gorur, A., Baumgärtel, C., Schekman, R. and Rape, M. (2012). Ubiquitin-dependent regulation of COPII coat size and function. *Nature* **482**, 495-500.

Korkut, C., Ataman, B., Ramachandran, P., Ashley, J., Barria, R., Gherbesi, N. and Budnik, V. (2009). Trans-synaptic transmission of vesicular Wnt signals through Evi/Wntless. *Cell* **139**, 393-404.

Kurayoshi, M., Yamamoto, H., Izumi, S. and Kikuchi, A. (2007). Post-translational palmitoylation and glycosylation of Wnt-5a are necessary for its signalling. *Biochem. J.* **402**, 515-523.

Li, Q., Jain, M.R., Chen, W., and Li, H. (2013). A multidimensional approach to an in-depth proteomics analysis of transcriptional regulators in neuroblastoma cells. *J. Neurosci. Methods*, **216**, 118-127.

Li, X., Wu, Y., Shen, C., Belenkaya, T. Y., Ray, L. and Lin, X. (2015). Drosophila p24 and Sec22 regulate Wingless trafficking in the early secretory pathway. *Biochem. Biophys. Res. Commun.* **463**, 483-489.

Liu, J., Pan, S., Hsieh, M. H., Ng, N., Sun, F., Wang, T., Kasibhatla, S., Schuller, A. G., Li, A. G., Cheng, D. et al. (2013). Targeting Wnt-driven cancer through the inhibition of Porcupine by LGK974. *Proc. Natl. Acad. Sci. USA* **110**, 20224-20229.

MacDonald, B. T., Tamai, K. and He, X. (2009). Wnt/beta-catenin signaling: components, mechanisms, and diseases. *Dev. Cell* **17**, 9-26.

MacDonald, B. T., Hien, A., Zhang, X., Iranloye, O., Virshup, D. M., Waterman, M. L. and He, X. (2014). Disulfide bond requirements for active Wnt ligands. *J. Biol. Chem.* **289**, 18122-18136.

Madan, B., Ke, Z., Harmston, N., Ho, S. Y., Frois, A. O., Alam, J., Jeyaraj, D. A., Pendharkar, V., Ghosh, K., Virshup, I. H. et al. (2016). Wnt addiction of genetically defined cancers reversed by PORCN inhibition. *Oncogene* **35**, 2197-2207.

McMahon, C., Studer, S. M., Clendinen, C., Dann, G. P., Jeffrey, P. D. and Hughson, F. M. (2012). The structure of Sec12 implicates potassium ion coordination in Sar1 activation. *J. Biol. Chem.* **287**, 43599-43606.

Montegna, E. A., Bhave, M., Liu, Y., Bhattacharyya, D. and Glick, B. S. (2012). Sec12 binds to Sec16 at transitional ER sites. *PLoS ONE* **7**, e31156.

Neer, E. J., Schmidt, C. J., Nambudripad, R. and Smith, T. F. (1994). The ancient regulatory-protein family of WD-repeat proteins. *Nature* **371**, 297-300.

Pan, C. L., Baum, P. D., Gu, M., Jorgensen, E. M., Clark, S. G. and Garriga, G. (2008). C. elegans AP-2 and retromer control Wnt signaling by regulating mig-14/Wntless. *Dev. Cell* **14**, 132-139.

Port, F., Kuster, M., Herr, P., Furger, E., Bänziger, C., Hausmann, G. and Basler, K. (2008). Wingless secretion promotes and requires retromer-dependent cycling of Wntless. *Nat. Cell Biol.* **10**, 178-185.

Port, F., Hausmann, G. and Basler, K. (2011). A genome-wide RNA interference screen uncovers two p24 proteins as regulators of Wingless secretion. *EMBO Rep.* **12**, 1144-1152.

Journal of Cell Science

Proffitt, K. D., Madan, B., Ke, Z., Pendharkar, V., Ding, L., Lee, M. A., Hannoush, R. N. and Virshup, D. M. (2013). Pharmacological inhibition of the Wnt acyltransferase PORCN prevents growth of WNT-driven mammary cancer. *Cancer Res.* **73**, 502-507.

Rojas, R., van Vlijmen, T., Mardones, G. A., Prabhu, Y., Rojas, A. L., Mohammed, S., Heck, A. J. R., Raposo, G., van der Sluijs, P. and Bonifacino, J. S. (2008). Regulation of retromer recruitment to endosomes by sequential action of Rab5 and Rab7. *J. Cell Biol.* **183**, 513-526.

Saito, K., Chen, M., Bard, F., Chen, S., Zhou, H., Woodley, D., Polischuk, R., Schekman, R. and Malhotra, V. (2009). TANGO1 facilitates cargo loading at endoplasmic reticulum exit sites. *Cell* **136**, 891-902.

Saito, K., Yamashiro, K., Shimazu, N., Tanabe, T., Kontani, K. and Katada, T. (2014). Concentration of Sec12 at ER exit sites via interaction with cTAGE5 is required for collagen export. *J. Cell Biol.* **206**, 751-762.

Sakamori, R., Das, S., Yu, S., Feng, S., Stypulkowski, E., Guan, Y., Douard, V., Tang, W., Ferraris, R. P., Harada, A. et al. (2012). Cdc42 and Rab8a are critical for intestinal stem cell division, survival, and differentiation in mice. *J. Clin. Invest.* **122**, 1052-1065.

Sakamori, R., Yu, S., Zhang, X., Hoffman, A., Sun, J., Das, S., Vedula, P., Li, G., Fu, J., Walker, F. et al. (2014). CDC42 inhibition suppresses progression of incipient intestinal tumors. *Cancer Res.* **74**, 5480-5492.

Sato, K. and Nakano, A. (2005). Dissection of COPII subunit-cargo assembly and disassembly kinetics during Sar1p-GTP hydrolysis. *Nat. Struct. Mol. Biol.* **12**, 167-174.

Schindelin, J., Arganda-Carreras, I., Frise, E., Kaynig, V., Longair, M., Pietzsch, T., Preibisch, S., Rueden, C., Saalfeld, S., Schmid, B. et al. (2012). Fiji: an open-source platform for biological-image analysis. *Nat. Methods* **9**, 676-682.

Schneider, C. A., Rasband, W. S. and Eliceiri, K. W. (2012). NIH Image to ImageJ: 25 years of image analysis. *Nat. Methods* **9**, 671-675.

Skehel, P. A., Fabian-Fine, R. and Kandel, E. R. (2000). Mouse VAP33 is associated with the endoplasmic reticulum and microtubules. *Proc. Natl. Acad. Sci. USA* **97**, 1101-1106.

Stirnimann, C. U., Petsalaki, E., Russell, R. B. and Muller, C. W. (2010). WD40 proteins propel cellular networks. *Trends Biochem. Sci.* **35**, 565-574.

Takada, R., Satomi, Y., Kurata, T., Ueno, N., Norioka, S., Kondoh, H., Takao, T. and Takada, S. (2006). Monounsaturated fatty acid modification of Wnt protein: its role in Wnt secretion. *Dev. Cell* **11**, 791-801.

Voloshanenko, O., Erdmann, G., Dubash, T. D., Augustin, I., Metzig, M., Moffa, G., Hundsrucker, C., Kerr, G., Sandmann, T., Anchang, B. et al. (2013). Wnt secretion is required to maintain high levels of Wnt activity in colon cancer cells. *Nat. Commun.* **4**, 2610.

Watson, P., Townley, A. K., Koka, P., Palmer, K. J. and Stephens, D. J. (2006). Sec16 defines endoplasmic reticulum exit sites and is required for secretory cargo export in mammalian cells. *Traffic* **7**, 1678-1687.

Wilhelmi, I., Kanski, R., Neumann, A., Herdt, O., Hoff, F., Jacob, R., Preussner, M. and Heyd, F. (2016). Sec16 alternative splicing dynamically controls COPII transport efficiency. *Nat. Commun.* **7**, 12347.

Willert, K., Brown, J. D., Danenberg, E., Duncan, A. W., Weissman, I. L., Reya, T., Yates, J. R., III and Nusse, R. (2003). Wnt proteins are lipid-modified and can act as stem cell growth factors. *Nature* **423**, 448-452.

Yang, P.-T., Lorenowicz, M. J., Silhankova, M., Coudreuse, D. Y., Betist, M. C. and Korswagen, H. C. (2008). Wnt signaling requires retromer-dependent recycling of MIG-14/Wntless in Wnt-producing cells. *Dev. Cell* **14**, 140-147.

Yoshihisa, T., Barlowe, C. and Schekman, R. (1993). Requirement for a GTPase-activating protein in vesicle budding from the endoplasmic reticulum. *Science* **259**, 1466-1468.

Yu, J., Chia, J., Canning, C. A., Jones, C. M., Bard, F. A. and Virshup, D. M. (2014a). WLS retrograde transport to the endoplasmic reticulum during Wnt secretion. *Dev. Cell* **29**, 277-291.

Yu, S., Nie, Y., Knowles, B., Sakamori, R., Stypulkowski, E., Patel, C., Das, S., Douard, V., Ferraris, R. P., Bonder, E. M. et al. (2014b). TLR sorting by Rab11 endosomes maintains intestinal epithelial-microbial homeostasis. *EMBO J.* **33**, 1882-1895.

Yu, S., Yehia, G., Wang, J., Stypulkowski, E., Sakamori, R., Jiang, P., Hernandez-Enriquez, B., Tran, T. S., Bonder, E. M., Guo, W. et al. (2014c). Global ablation of the mouse Rab11a gene impairs early embryogenesis and matrix metalloproteinase secretion. *J. Biol. Chem.* **289**, 32030-32043.

Zhang, P., Zhou, L., Pei, C., Lin, X. and Yuan, Z. (2016). Dysfunction of Wntless triggers the retrograde Golgi-to-ER transport of Wingless and induces ER stress. *Sci. Rep.* **6**, 19418.

Zhuang, X., Chowdhury, S., Northup, J. K. and Ray, K. (2010). Sar1-dependent trafficking of the human calcium receptor to the cell surface. *Biochem. Biophys. Res. Commun.* **396**, 874-880.